JACS
JOURNAL OF THE AMERICAN CHEMICAL SOCIETY
Communication
pubs.acs.org/JACS

Influence of Regio- and Chemoselectivity on the Properties of Fluoro-Substituted Thienothiophene and Benzodithiophene Copolymers

Hongliang Zhong,[†] Chang-Zhi Li,[†] Joshua Carpenter,[§] Harald Ade,[§] and Alex K.-Y. Jen*[,†,‡]

[†]Department of Materials Science & Engineering and [‡]Department of Chemistry, University of Washington, Seattle, Washington 98195, United States

[§]Department of Physics, North Carolina State University, Raleigh, North Carolina 27695, United States

Supporting Information

ABSTRACT: By studying the regio- and chemoselectivity of fluoro-substituted thienothiophene and benzodithiophene copolymers, we found polymers made from conventional one-pot polycondensation reaction consist of two distinctly different segments with a ratio of 0.36/0.64. Through further comparative studies of neat regioregular polymers based on each individual segment, we have identified the specific segment that contributes to the superior absorption, packing order, and charge mobility in the corresponding polymers. The unique structure−property relationships are the result of cooperative molecular arrangements of the key segment and noncovalent interaction between the fluoro group and the aromatic proton on the thiophene side-chain of the polymers.

Donor−acceptor (D−A) conjugated polymers with alternating electron-rich (donor) and electron-deficient (acceptor) units have been widely employed as crucial components for organic electronics.[1−6] Over the past few years, a large number of conjugated copolymers have been developed, with the focus of the studies emphasized primarily on tuning their optical and electronic properties by varying the D−A combinations.[7,8] Since these copolymers are commonly synthesized through one-pot polycondensation reaction between the corresponding D and A monomers, an unresolved complex issue is to define the actual polymer structure arising from the different regio- and chemoselectivity of the reactive intermediates during polymerization.[9,10] For instance, homocoupling of monomer occurs sometimes resulting in structural defects of polymers.[11,12] The situation becomes even more complicated when asymmetric monomers are involved in polymerization, bringing the issue of regioregularity in the resultant polymers.[13,14] Previous studies have demonstrated that regioregular polymer affords enhanced solid-state packing order, which results in significantly increased charge-transporting properties than those obtained from regiorandom polymer of the same compositions.[13−16] Although these structural factors affect polymer optoelectronic properties, they are often neglected. Therefore, clear structure−property relationships between these aspects need to be established to facilitate rational design of efficient D−A conjugated polymers.

Among the reported D−A conjugated polymers, PBDT-FTT analogues comprising benzodithiophene (BDT) and fluoro-substituted thieno[3,4-*b*]thiophene (FTT) moieties are very attractive for their capability of producing high efficiencies in organic photovoltaics (OPVs).[17−19] For example, polymer PTB7 shows a high power conversion efficiency (PCE) of 7−9%.[20] After replacing the alkoxy group in BDT with the alkyl substituted thiophene (BDTT), a new polymer PTB7-Th can reach ∼10% PCE.[21−24] Nevertheless, a critical challenge that remains unsolved is the undefined backbone structures for these polymers. This is due to the specific regio- and chemopreference of asymmetric FTT affecting the reaction rate during the polymerization. The undetermined structures hinder the deeper understanding of the structure−property relationships in PBDT-FTT polymers, which prevents the rapid development of new superior materials.

In this work, the commonly studied PTB7-Th was employed as the representative polymer in the PBDT-FTT family to reveal that two segments (with a ratio of 0.36/0.64) were formed from the routine polycondensation reaction. This structural feature originates from the exclusive regioselectivity at the 6-position of the asymmetric FTT, and the preferential chemoselectivity to form an A−D−A intermediate during polymerization. More importantly, the studies of regioregular polymers based on 100% individual segment show that it correlates well with the improved polymer absorption, solid-state packing, and charge mobility. This structure−property relationship is derived from the cooperative effect of unique molecular arrangement and the weak interactions between the fluoro atom and the side-chains on polymers.

Since the structural diversity of PTB7-Th is mainly caused by FTT that possesses two asymmetric reactive sites at 4- and 6-positions (see Scheme 1), the regioselectivity of FTT is studied. The M0 (D−A−D) was first made by utilizing 1 equiv (eq) of FTT and 2 eq of BDTT in a Stille coupling reaction to serve as the reference because it possesses well-defined structure where both the 4- and 6-positions of FTT are substituted with BDTT. Then, the ratio of FTT to BDTT in the Stille reaction was increased to 1:1 and 2:1 so that only one of the FTT positions was substituted to form M1 (D−A) and M2 (A−D−A), respectively. As seen in Figure S1, the ^{1}H NMR spectrum of

Received: April 22, 2015
Published: May 29, 2015

DOI: 10.1021/jacs.5b04209
J. Am. Chem. Soc. 2015, 137, 7616−7619

Scheme 1. Synthetic Routes for Monomers M0, M1, and M2

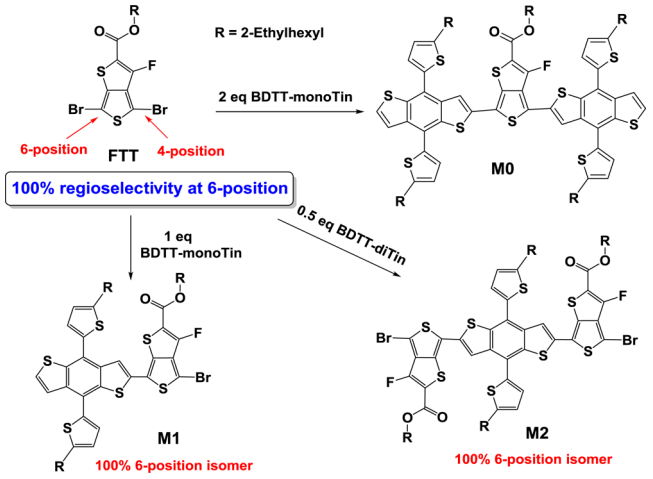

M0 shows two thiophene protons (H1 and H2) adjacent to FTT exhibit two different singlet signals, in which the peak at 8.01 ppm in lower field is attributed to the H1 located at the same side of the F atom, while the H2 peak is at 7.77 ppm. Surprisingly, only the singlet peaks of H3 (~7.94 ppm) and H4 (~7.90 ppm) appear for M1 and M2, suggesting only one isomer is formed in M1 and M2. The chemical shifts of H3 and H4 move to lower field relative to H2, which fit the less electron-rich nature of M1 and M2, indicating FTT in M1 and M2 are exclusively substituted at its 6-position. This is consistent with the high regioselectivity of thieno[3,4-*b*]thiophene derivative observed in previous reports.[25]

On the basis of the exclusive regioselectivity of FTT, there are two potential routes for the initial stage polymerization of PTB7-Th, leading to two different segments, namely, as unit A and unit B. As shown in Scheme 2a, both BDTT-diTin and FTT would be consumed at the same rate to convert into M1-Tin, which further polymerizes to form unit A-rich regioregular polymer (P1) in route 1. In route 2, BDTT-diTin will react with 2 eq of FTT initially to form M2, leaving an identical amount of unreacted BDTT-diTin. The subsequent polymerization will yield unit B-rich regioregular polymer (P2). During polymerization, these two routes may proceed simultaneously and compete against each other. However, the chemoselectivity of polymerization on the choice of route 1 and/or route 2, which determines the ratio between units A and B in PTB7-Th, is still unclear. Therefore, NMR spectroscopy was used to estimate this; however, it failed due to overlapped broad proton signals of the polymers.

Noting the possible polymerization pathways revealed that the amount of M2 formed should be equal to that of the unreacted BDTT-diTin at the very moment FTT is completely consumed. As shown in Scheme 2b, a model polymerization reaction was conducted under the same conditions[21] reported for preparing PTB7-Th except using different solvent. Since the addition of DMF is known to accelerate the Stille coupling reaction,[10] only toluene was utilized in the model reaction to facilitate the monitoring of reaction. By monitoring with thin layer chromatography (TLC), the model reaction was terminated as soon as the FTT was fully consumed (see SI for details). Along with various oligomers, 0.32 eq of nonpolar BDTT was facilely recovered, which indicates at least 0.32 eq of M2 (A−D−A) was formed at the initial stage then completely converted into segment B (D−A−D−A). It suggests that 64% (0.32 × 2) of the total BDTT-diTin (D) and FTT (A) adopt the route 2 at the initial stage of polymerization, leading to more than 64% of unit B as the dominant segment in PTB7-Th.

Based on this structural information, the studies were directed to identify the influences of units A and B on polymer properties. Three polymers with different backbone regioregularity were synthesized from the corresponding monomers under the same conditions. P1 and P2 comprise the neat unit A and unit B on their backbones, respectively. P3 is prepared from the same procedure reported for commonly used PTB7-Th,[21] which consists of 36% unit A and 64% unit B as shown. The polymer structures are displayed in Scheme 2, and experimental details are in SI. These polymers show good and comparable molecular weight (M_n) and polydispersity index (PDI), 73 kDa/2.3, 78 kDa/1.5, and 56 kDa/1.5 for P1, P2, and P3, respectively.

Scheme 2. (a) Possible Pathways for PTB7-Th Polymerization; (b) Model Polymerization of PTB7-Th

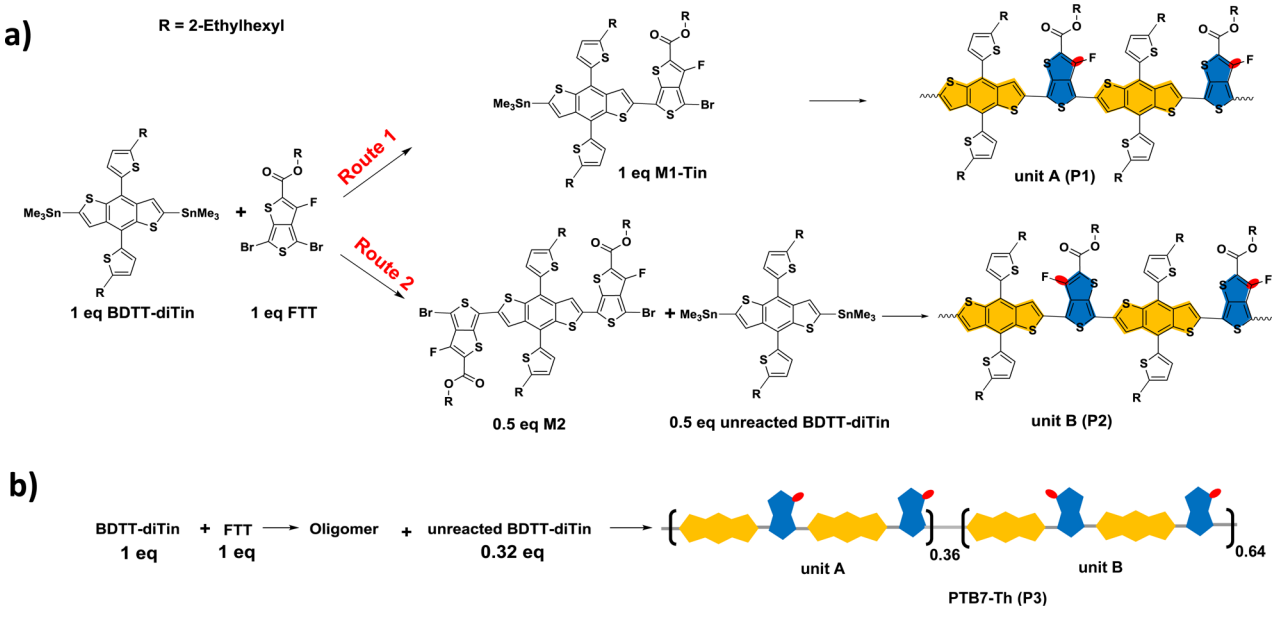

DOI: 10.1021/jacs.5b04209
J. Am. Chem. Soc. 2015, 137, 7616−7619

The chemical structures of these polymers were characterized by ^{1}H NMR spectroscopy. As above-mentioned, it is difficult to distinguish the features for units A and B in NMR spectra due to overlapped signals. As shown in Figure S2, P1 and P2 show significantly different signals around 7.45 and 7.05 ppm, which correspond to the aromatic protons on the thiophene side-chains. There are obvious shoulder peaks adjacent to the main peaks in the NMR spectrum of P1, indicating the interaction exists with the thiophene side-chains, which leads to varied chemical environments for these protons. These protons on P2 appear to be two different peaks with similar intensities, suggesting that the interaction has more influence on P2 compared to P1. The NMR spectrum of P3 shows features from both P1 and P2. The interaction on thiophene side-chains can be further elucidated by studying the effect of fluorination.

To study the influence of varied repeat units on molecular arrangements of P1, P2, and P3, the UV–vis absorption spectra are acquired for these three polymers in dilute solution, and the results are shown in Figure 1a. All three polymers exhibit

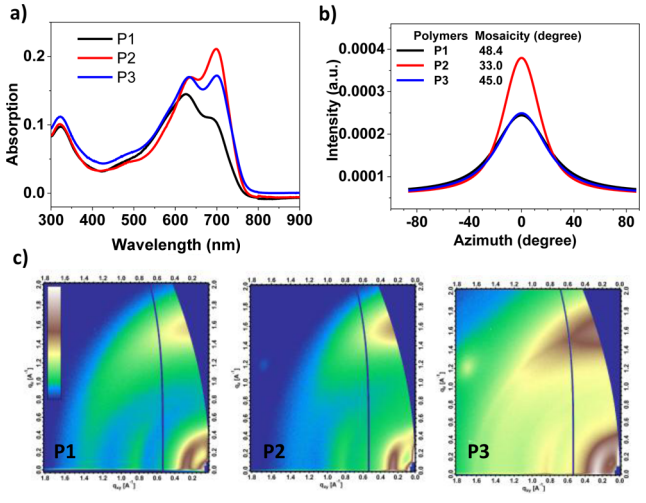

Figure 1. (a) UV–vis absorption spectra in 5×10^{-6} M dichlorobenzene solution. (b) Voigt profiles, which were fitted to pole figures obtained by processing the 2-dimensional GIWAXS data for P1, P2, and P3 shown in panel c.

intramolecular charge transfer (ICT) peaks (~630 nm) and aggregation peaks (~700 nm). However, the ICT peaks of P2 and P3 show ~17% enhanced intensities compared to that of P1, indicating unit B-rich polymers P2 and P3 have higher effective conjugation lengths. Moreover, significantly different aggregation-induced peaks are also observed in which P1 displays the weakest aggregation peak among all three polymers, while the peak in P2 is the strongest with 2- and 1.2-fold higher intensity compared to those of P1 and P3, respectively. These absorption features suggest that the planarity and chain packing of polymers are gradually enhanced with the increasing ratio of unit B in the polymers.

To further investigate the chain packing of polymers, grazing-incidence wide-angle X-ray scattering (GIWAXS) was performed on spin-coated pristine polymer films. As shown in Figure 1c, all three polymers show preferable face-on crystalline orientation and out-of-plane π–π stacking, but the diffraction peaks for P1 and P3 show relatively broad distributions in azimuth compared with those of P2. The mosaicity of π–π stacking peaks is quantified to analyze their orientation disorder of the crystallite in each film (see SI for details of the GIWAXS data analysis). Figure 1b shows the mosaicity of these three polymers, 48.4°, 33.0°, and 45.0° for P1, P2 and P3, respectively, indicating P2 has the highest order of orientation, while P1 has the lowest. Moreover, field-effect transistors (FETs) were used to evaluate charge-transporting characteristics of these polymers because charge mobility of polymers is significantly affected by their structural planarity and solid-state packing order. As shown in Figure S3, P1 shows a hole-mobility of 2.0×10^{-3} cm^2 V^{-1} s^{-1}, while the mobility of P2 (1.5×10^{-2} cm^2 V^{-1} s^{-1}) is almost 1 order of magnitude higher than that of P1 and P3 (5.7×10^{-3} cm^2 V^{-1} s^{-1}). These results are in good agreement with the features observed in UV–vis absorption and GIWAXS measurements. This indicates that structural diversity of unit A and unit B strongly affects polymer properties in both solid-state and solution.

Especially, the ratio of unit B in polymer backbone (in the order of P1 < P3 < P2) leads to stronger absorption, improved packing order, and higher charge mobility. Comparing two segments, unit A and unit B, the main difference lies on the orientation of FTT unit and F-directing point. In these structures, the fluoro atoms play an important role in determining polymer conformation through noncovalent interaction, in addition to influencing the frontier orbitals of polymers.[26,27] Liu et al. have previously found that the OPV efficiency improved with the increasing F-content in PTB7-Th;[28] however, He et al. have also suggested that the F-dependent effect is less obvious in PTB7 case.[29] Note that the major difference between PTB7 and PTB7-Th are the side-chains on the BTT unit. Clarifying the correlation between these interesting observations will benefit the design of future superior materials.

The effect of fluorination on polymer conformation is further studied, in particular for the side-chain rotation, by using dynamic proton NMR. Because polymers are not suitable for these studies due to indistinguishable proton signals at low temperature, model compound M0 is employed for this investigation. It has one BDTT unit adjacent to the FTT fluoro atom, while the other one is located at the opposite side. As shown in Figure 2, the aromatic protons e1 and e2 on the thiophene side-chains near the fluoro atom split from one peak (0 °C) to two different peaks (below −10 °C) with decreased temperature. On the contrary, e3 and e4 of the other BDTT at the opposite side of the fluoro atom remain one peak with only a slight shift under varied temperatures. The large change of chemical shift precludes the possibility of a spin–spin coupling caused doublet, indicating e1 and e2 are actually under different chemical environments (for instance, e1 is interacting with fluoro atom, whereas e2 is not). In addition, Figure S4 also shows the temperature-dependent ^{19}F NMR spectra, in which the peak becomes broadened by judging from the change of full width at half-maximum (fwhm) when the temperature was gradually decreased from 0 to −30 °C. These features found in dynamic NMR suggest that a weak noncovalent interaction is present between the fluoro atom on FTT and the aromatic proton of thiophene side-chain on BDTT, which is in good agreement with the NMR spectra of polymers.This result also explains the effect of different fluoro content on PTB7-Th and PTB7 performance due to the lack of aromatic side-chains in the latter. Although this interaction presents in both unit A and B, P1 and P2 show significantly different properties, which may be rationalized by their different polymer backbone architecture. As shown in Figure S5, each BDTT unit in P1 interacts with only one fluoro atom, whereas half the numbers of BDTT units are

DOI: 10.1021/jacs.5b04209
J. Am. Chem. Soc. 2015, 137, 7616–7619

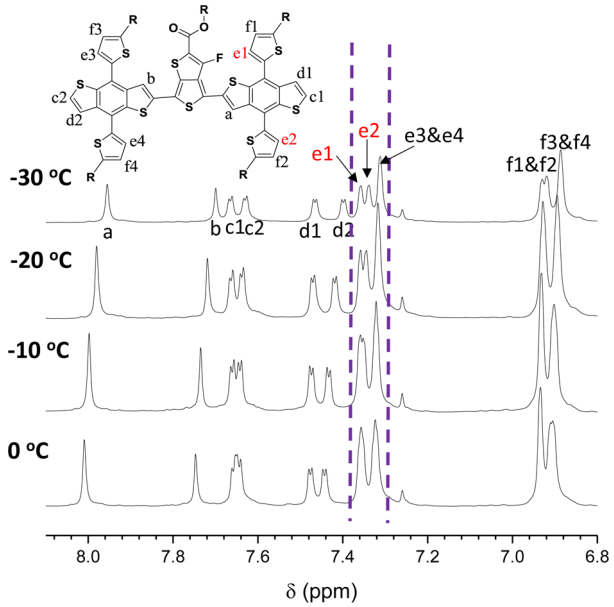

Figure 2. Dynamic ^{1}H NMR of M0 in deuterated chloroform solution (30 mg/mL).

simultaneously affected by two fluoro atoms in P2, indicating both thiophene side-chains were locked locally.

In conclusion, we have employed an integrative chemical approach to systematically investigate the regioselectivity and chemoselectivity in PTB7-Th polymerization. The methodology detailed here provides considerable insights to study other polymer classes containing asymmetric monomers. Based on the studies of model monomers and reactions, we reveal that the commonly used PTB7-Th from one-pot polymerization consists of two major segments, in which the dominant one exceeds 64% in overall content. Interestingly, the higher ratio of this key segment in polymer leads to superior absorption, ordered packing, and charge mobility. Dynamic NMR studies further verify the presence of noncovalent interactions between the fluoro atom of the FTT and the thiophene side-chain of BDTT, resulting in a more rigid and planar structure of dominant segment. These studies help elucidating the structure−property relationships of high performance polymers to provide new insights for rational design of superior optoelectronic materials.

■ ASSOCIATED CONTENT

Ⓢ Supporting Information

Experimental details for the synthesis and supplementary figures. The Supporting Information is available free of charge on the ACS Publications website at DOI: 10.1021/jacs.5b04209.

■ AUTHOR INFORMATION

Corresponding Author

*ajen@u.washington.edu

Notes

The authors declare no competing financial interest.

■ ACKNOWLEDGMENTS

The authors thank the support from the AOARD (No. FA2386-11-1-4072), the ONR (No. N00014-14-1-0170). A.K.-Y.J. thanks the Boeing Foundation for support. X-ray characterization by NCSU was supported by the ONR (No. N000141410531). X-ray data were acquired at beamline 7.3.3, the Advanced Light Source, which is supported by the Director, Office of Science, Office of Basic Energy Sciences, of the U.S. Department of Energy under Contract No. DE-AC02-05CH11231. The authors thank Mr. Shengqiang Liu for the OFET characterization and Dr. Adrienne Roehrich for the help of NMR measurement.

■ REFERENCES

(1) Cheng, Y.-J.; Yang, S.-H.; Hsu, C.-S. *Chem. Rev.* **2009**, *109*, 5868.
(2) Beaujuge, P. M.; Fréchet, J. M. J. *J. Am. Chem. Soc.* **2011**, *133*, 20009.
(3) Li, Y. *Acc. Chem. Res.* **2012**, *45*, 723.
(4) Duan, C.; Huang, F.; Cao, Y. *J. Mater. Chem.* **2012**, *22*, 10416.
(5) Guo, X.; Baumgarten, M.; Müllen, K. *Prog. Polym. Sci.* **2013**, *38*, 1832.
(6) Liu, Y.; Zhao, J.; Li, Z.; Mu, C.; Ma, W.; Hu, H.; Jiang, K.; Lin, H.; Ade, H.; Yan, H. *Nat. Commun.* **2014**, *5*, 5293.
(7) Po, R.; Bianchi, G.; Carbonera, C.; Pellegrino, A. *Macromolecules* **2015**, *48*, 453.
(8) Zhou, H.; Yang, L.; You, W. *Macromolecules* **2012**, *45*, 607.
(9) Coffin, R. C.; Peet, J.; Rogers, J.; Bazan, G. C. *Nat. Chem.* **2009**, *1*, 657.
(10) Carsten, B.; He, F.; Son, H. J.; Xu, T.; Yu, L. *Chem. Rev.* **2011**, *111*, 1493.
(11) Lu, L.; Zheng, T.; Xu, T.; Zhao, D.; Yu, L. *Chem. Mater.* **2015**, *27*, 537.
(12) Hendriks, K. H.; Li, W.; Heintges, G. H. L.; van Pruissen, G. W. P.; Wienk, M. M.; Janssen, R. A. J. *J. Am. Chem. Soc.* **2014**, *136*, 11128.
(13) Steyrleuthner, R.; Di Pietro, R.; Collins, B. A.; Polzer, F.; Himmelberger, S.; Schubert, M.; Chen, Z.; Zhang, S.; Salleo, A.; Ade, H.; Facchetti, A.; Neher, D. *J. Am. Chem. Soc.* **2014**, *136*, 4245.
(14) Ying, L.; Hsu, B. B. Y.; Zhan, H.; Welch, G. C.; Zalar, P.; Perez, L. A.; Kramer, E. J.; Nguyen, T.-Q.; Heeger, A. J.; Wong, W.-Y.; Bazan, G. C. *J. Am. Chem. Soc.* **2011**, *133*, 18538.
(15) McCulloch, I.; Heeney, M.; Bailey, C.; Genevicius, K.; MacDonald, I.; Shkunov, M.; Sparrowe, D.; Tierney, S.; Wagner, R.; Zhang, W.; Chabinyc, M. L.; Kline, R. J.; McGehee, M. D.; Toney, M. F. *Nat. Mater.* **2006**, *5*, 328.
(16) Sirringhaus, H.; Brown, P. J.; Friend, R. H.; Nielsen, M. M.; Bechgaard, K.; Langeveld-Voss, B. M. W.; Spiering, A. J. H.; Janssen, R. A. J.; Meijer, E. W.; Herwig, P.; de Leeuw, D. M. *Nature* **1999**, *401*, 685.
(17) Liang, Y.; Feng, D.; Wu, Y.; Tsai, S.-T.; Li, G.; Ray, C.; Yu, L. *J. Am. Chem. Soc.* **2009**, *131*, 7792.
(18) Liang, Y.; Xu, Z.; Xia, J.; Tsai, S.-T.; Wu, Y.; Li, G.; Ray, C.; Yu, L. *Adv. Mater.* **2010**, *22*, E135.
(19) Ye, L.; Zhang, S.; Huo, L.; Zhang, M.; Hou, J. *Acc. Chem. Res.* **2014**, *47*, 1595.
(20) He, Z.; Zhong, C.; Su, S.; Xu, M.; Wu, H.; Cao, Y. *Nat. Photonics* **2012**, *6*, 591.
(21) Liao, S.-H.; Jhuo, H.-J.; Cheng, Y.-S.; Chen, S.-A. *Adv. Mater.* **2013**, *25*, 4766.
(22) Liao, S.-H.; Jhuo, H.-J.; Yeh, P.-N.; Cheng, Y.-S.; Li, Y.-L.; Lee, Y.-H.; Sharma, S.; Chen, S.-A. *Sci. Rep.* **2014**, *4*, 6813.
(23) He, Z.; Xiao, B.; Liu, F.; Wu, H.; Yang, Y.; Xiao, S.; Wang, C.; Russell, T. P.; Cao, Y. *Nat. Photonics* **2015**, *9*, 174.
(24) Liu, C.; Yi, C.; Wang, K.; Yang, Y.; Bhatta, R. S.; Tsige, M.; Xiao, S.; Gong, X. *ACS Appl. Mater. Interfaces* **2015**, *7*, 4928.
(25) Zhang, C.; Zang, Y.; Gann, E.; McNeill, C. R.; Zhu, X.; Di, C.-a.; Zhu, D. *J. Am. Chem. Soc.* **2014**, *136*, 16176.
(26) Li, W.; Albrecht, S.; Yang, L.; Roland, S.; Tumbleston, J. R.; McAfee, T.; Yan, L.; Kelly, M. A.; Ade, H.; Neher, D.; You, W. *J. Am. Chem. Soc.* **2014**, *136*, 15566.
(27) Nguyen, T. L.; Choi, H.; Ko, S. J.; Uddin, M. A.; Walker, B.; Yum, S.; Jeong, J. E.; Yun, M. H.; Shin, T. J.; Hwang, S.; Kim, J. Y.; Woo, H. Y. *Energy Environ. Sci.* **2014**, *7*, 3040.
(28) Liu, P.; Zhang, K.; Liu, F.; Jin, Y.; Liu, S.; Russell, T. P.; Yip, H.-L.; Huang, F.; Cao, Y. *Chem. Mater.* **2014**, *26*, 3009.
(29) He, X.; Mukherjee, S.; Watkins, S.; Chen, M.; Qin, T.; Thomsen, L.; Ade, H.; McNeill, C. R. *J. Phys. Chem. C* **2014**, *118*, 9918.

DOI: 10.1021/jacs.5b04209
J. Am. Chem. Soc. 2015, 137, 7616−7619